JOURNAL OF COMPUTATIONAL PHYSICS 67, 310–326 (1986)

The Use of Symmetry in Bifurcation Calculations and Its Application to the Bénard Problem

K. A. CLIFFE AND K. H. WINTERS

Theoretical Physics Division, Building 424.4, AERE Harwell, Oxon OX11 ORA, England

Received October 16, 1984; revised March 14, 1986

Some aspects of the use of symmetry in bifurcation calculations are discussed. First, it is shown how substantial reductions in cost are obtained in computing symmetry-breaking bifurcation points by exploiting the underlying symmetry of a problem. This is demonstrated in a finite-element calculation of 2-dimensional Bénard convection in a finite cavity. Second, the stability of paths of symmetry-breaking bifurcation points, which occur when a second parameter in the problem varies, is investigated. A criterion is established for deciding whether intersection of such paths is allowed by symmetry constraints.

1. INTRODUCTION

In some recent papers [1–4] we have studied certain bifurcation problems in fluid flow by using extended systems of steady state equations. The solution of an extended system gives the location of a bifurcation point as well as the solution of the original equations at that point. The choice of extended system depends on the type of bifurcation point under consideration. In the case of symmetry-breaking bifurcations in the Bénard and Taylor problems, we applied an algorithm due to Moore [5] for which Newton's method was found to give rapid convergence. However, this technique is unnecessarily inefficient, since one must solve the equations over the entire domain; no account is taken of the symmetry which is broken at the bifurcation.

Recently, Werner and Spence [6] have proposed a method for finding symmetry-breaking bifurcation points which uses explicitly the underlying symmetry of the problem; the computation is carried out in the subdomain over which the solution posseses the symmetry which is broken at the bifurcation. This offers a substantial saving in computation time, reducing the number of degrees of freedom by a factor of 4 in two dimensions. One purpose of the present paper is to show how the Werner–Spence algorithm may be implemented in a finite element formulation and applied to the 2-dimensional problem of Bénard convection in a cavity. The cost of the computation is found to be reduced by a factor of 10 in comparison to the Moore algorithm which takes no account of symmetry. This reduction is to be expected in calculations using a direct solution method as here.

0021-9991/86 $3.00

The Werner-Spence algorithm provides a general technique for locating symmetry-breaking bifurcation points on an arbitrary solution branch. In Bénard convection, the bifurcation is actually from the trivial solution, and we derive an algorithm which exploits the special nature of this type of problem. This is found to give a further cost reduction of one half.

Once the value of a parameter at which there is a bifurcation has been found, one is usually interested in finding how this value varies as a second parameter is changed. For example, in Bénard convection in a closed cavity, the critical value of Rayleigh number is frequently computed as a function of the aspect ratio of the cavity. In this way a path of symmetry-breaking bifurcation points is traced out in the 2-parameter space. The question which then arises is what happens when this path crosses a second path of symmetry-breaking bifurcation points? In the Bénard problem described, it is found empirically that such paths sometimes cross and sometimes avoid crossing; for Bénard convection in a cylinder the paths always avoid intersecting. A second aim of this paper is to establish a criterion for deciding whether or not paths of symmetry-breaking bifurcation points in a 2-parameter problem can cross in a stable way.

Finally, we point out an important feature of finite-element calculations of Bénard convection. Most of the commonly used elements produce a spurious source of momentum; this leads to errors of several percent in the predicted critical Rayleigh number, unless exceptionally fine meshes are used. The present computations were carried out with a particular element, with piecewise-linear approximation of the pressure and quadratic velocities and temperature, which removes this problem.

2. Extended Systems

2.1. *Symmetry-Breaking Bifurcation Points and Their Computation*

In this section we summarize the theory of symmetry-breaking bifurcation points and describe algorithms for their computation. The material here relies heavily on Werner and Spence [6] and Werner [7].

We are concerned with nonlinear problems which depend on two parameters:

$$\mathbf{f}(\mathbf{x}, \lambda, \mu) = 0, \qquad \mathbf{f}: \mathbf{X} \times R \times R \to \mathbf{X} \tag{2.1}$$

where $\mathbf{x}$ is a state variable, λ and μ are real parameters, and $\mathbf{f}$ is a smooth mapping on a Banach space $\mathbf{X}$. We assume that $\mathbf{f}$ satisfies the symmetry relation

$$\mathbf{f}(\gamma\mathbf{x}, \lambda, \mu) = \gamma\mathbf{f}(\mathbf{x}, \lambda, \mu), \qquad \mathbf{x} \in \mathbf{X},\ \lambda, \mu \in R,\ \gamma \in \Gamma \tag{2.2}$$

where Γ is a representation over $\mathbf{X}$ of the group $\mathbf{Z}_2 \times \mathbf{Z}_2$. A physical example of this symmetry is given in Section 3 by Eqs. (3.8) and (3.9). We let the two generators of

Γ be α and β so that $\Gamma = \{I, \alpha, \beta, \alpha\beta\ (\equiv \beta\alpha)\}$. The mappings α and β introduce a natural decomposition of $\mathbf{X}$ into

$$\mathbf{X} = \mathbf{X}_{ss} \oplus \mathbf{X}_{sa} \oplus \mathbf{X}_{as} \oplus \mathbf{X}_{aa} \tag{2.3a}$$

where

$$\begin{aligned} \mathbf{X}_{ss} &= \{\mathbf{x} \in \mathbf{X} \mid \alpha\mathbf{x} = \mathbf{x},\ \beta\mathbf{x} = \mathbf{x}\} \\ \mathbf{X}_{sa} &= \{\mathbf{x} \in \mathbf{X} \mid \alpha\mathbf{x} = \mathbf{x},\ \beta\mathbf{x} = -\mathbf{x}\} \\ \mathbf{X}_{as} &= \{\mathbf{x} \in \mathbf{X} \mid \alpha\mathbf{x} = -\mathbf{x},\ \beta\mathbf{x} = \mathbf{x}\} \\ \mathbf{X}_{aa} &= \{\mathbf{x} \in \mathbf{X} \mid \alpha\mathbf{x} = -\mathbf{x},\ \beta\mathbf{x} = -\mathbf{x}\}. \end{aligned} \tag{2.3b}$$

The point $(\mathbf{x}_0, \lambda_0, \mu_0)$ is a singular point of (2.1) if $\mathbf{f}_{\mathbf{x}}^0 = \mathbf{f}_{\mathbf{x}}(\mathbf{x}_0, \lambda_0, \mu_0)$ is singular, otherwise $(\mathbf{x}_0, \lambda_0, \mu_0)$ is a regular point. A singular point is simple if there exists $\boldsymbol{\phi}_0 \in \mathbf{X}$, $\boldsymbol{\psi}_0 \in \mathbf{X}'$ (the dual of $\mathbf{X}$) such that

$$\text{Null}(\mathbf{f}_{\mathbf{x}}^0) = \text{Span}\{\boldsymbol{\phi}_0\}; \qquad \text{Range}(\mathbf{f}_x^0) = \{\mathbf{y} \in \mathbf{X} \mid \boldsymbol{\psi}_0\mathbf{y} = 0\}. \tag{2.4}$$

It is easy to show that, if $\mathbf{x}_0 \in \mathbf{X}_{ss}$, then $\boldsymbol{\phi}_0$ belongs to only one of $\mathbf{X}_{ss}$, $\mathbf{X}_{sa}$, $\mathbf{X}_{as}$, or $\mathbf{X}_{aa}$. We shall only consider the case $\boldsymbol{\phi}_0 \notin \mathbf{X}_{ss}$, that is, the symmetry-breaking case. Under the above assumptions it can be shown that

$$\boldsymbol{\psi}_0\mathbf{x} = 0 \qquad \text{for all} \quad \mathbf{x} \in \mathbf{X}_{ss}. \tag{2.5}$$

We consider first the case μ fixed, i.e.,

$$\mathbf{g}(\mathbf{x}, \lambda) = \mathbf{f}(\mathbf{x}, \lambda, \mu) = 0. \tag{2.6}$$

It is easy to show using (2.5) and $\boldsymbol{\phi}_0$ belongs to one of $\mathbf{X}_{sa}$, $\mathbf{X}_{as}$, $\mathbf{X}_{aa}$ that

$$\boldsymbol{\psi}_0\mathbf{g}_\lambda^0 = 0, \qquad \boldsymbol{\psi}_0\mathbf{g}_{\mathbf{xx}}^0\boldsymbol{\phi}_0\boldsymbol{\phi}_0 = 0. \tag{2.7}$$

Standard bifurcation theory now gives that $(\mathbf{x}_0, \lambda_0)$ is a pitchfork bifurcation point of (2.6) if and only if

$$\boldsymbol{\psi}_0(\mathbf{g}_{\lambda\mathbf{x}}^0\boldsymbol{\phi}_0 + \mathbf{g}_{\mathbf{xx}}^0\boldsymbol{\phi}_0\mathbf{v}) \neq 0, \tag{2.8}$$

where

$$\mathbf{g}_{\mathbf{x}}^0\mathbf{v} + \mathbf{g}_\lambda^0 = 0, \qquad \mathbf{v} \in \mathbf{X}_{ss}.$$

The familiar bifurcation diagram for this case is shown in Fig. 1.

Werner and Spence [6] showed how such points could be computed in a stable and efficient way. They proved that the extended system

$$\mathbf{G}(\mathbf{y}) = \begin{pmatrix} \mathbf{g}(\mathbf{x}, \lambda) \\ \mathbf{g}_{\mathbf{x}}(\mathbf{x}, \lambda)\boldsymbol{\phi} \\ /\boldsymbol{\phi} - 1 \end{pmatrix} = 0, \qquad \begin{aligned} &\mathbf{y} = (\mathbf{x}, \boldsymbol{\phi}, \lambda) \in \mathbf{Y}, \\ &\mathbf{Y} = \mathbf{X}_{ss} \times \mathbf{X}_1 \times R, \\ &\mathbf{G}: \mathbf{Y} \to \mathbf{Y} \end{aligned} \tag{2.9}$$

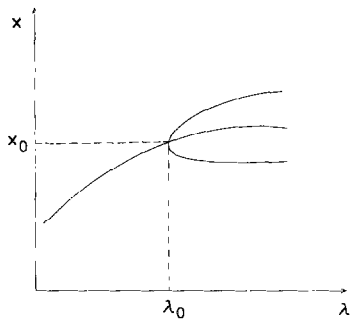

FIG. 1. Bifurcation diagram showing the symmetry-breaking bifurcation point (x_0, λ_0).

where $l \in \mathbf{X}'$ and $\mathbf{X}_1$ is one of $\mathbf{X}_{sa}$, $\mathbf{X}_{as}$, $\mathbf{X}_{aa}$ depending on which $\boldsymbol{\phi}_0$ belongs to, has an isolated solution at $(\mathbf{x}_0, \boldsymbol{\phi}_0, \lambda_0)$, if and only if $(\mathbf{x}_0, \lambda_0)$ is a symmetry-breaking bifurcation point. This result means that Newton's method may be used to solve (2.9). In [6] Werner and Spence discussed its implementation and gave several examples of algebraic and ordinary differential equations which exhibit $\mathbf{Z}_2$ and $\mathbf{Z}_2 \times \mathbf{Z}_2$ symmetry. Using the $\mathbf{Z}_2$ symmetry reduces the number of degrees of freedom in the discrete problem by about half; we shall show in the next section that the $\mathbf{Z}_2 \times \mathbf{Z}_2$ symmetry can be used to reduce the number of freedoms by about a factor four.

We now consider two parameter problems and introduce the extended system corresponding to (2.9)

$$\mathbf{F}(\mathbf{y}, \mu) = \begin{pmatrix} \mathbf{f}(\mathbf{x}, \lambda, \mu) \\ \mathbf{f}_{\mathbf{x}}(\mathbf{x}, \lambda, \mu)\boldsymbol{\phi} \\ l\boldsymbol{\phi} - 1 \end{pmatrix} = \mathbf{0} \qquad \begin{matrix} \mathbf{y} = (\mathbf{x}, \boldsymbol{\phi}, \lambda) \\ \\ \mathbf{F} : \mathbf{Y} \times R \to \mathbf{Y}. \end{matrix} \tag{2.10}$$

If (2.8) holds then $(\mathbf{y}, \mu_0)$ is a regular point of (2.10) and the implicit function theorem ensures that there is a neighbourhood of $(\mathbf{y}_0, \mu_0)$ in which $\mathbf{y}$ can be parametrized by μ. Hence standard continuation methods can be used to compute a path of symmetry-breaking bifurcation points.

If there is a trivial solution for all values of λ, μ, i.e., $\mathbf{f}(\mathbf{x}_0, \lambda, \mu) = 0$ for all λ and μ, then (2.10) simplifies to

$$\begin{pmatrix} \mathbf{f}_{\mathbf{x}}(\mathbf{x}_0, \lambda, \mu)\boldsymbol{\phi} \\ l\boldsymbol{\phi} - 1 \end{pmatrix} = \mathbf{0} \tag{2.10a}$$

and this can be used to calculate bifurcation from the trivial solution. Bénard convection is one example where this algorithm can be applied.

2.2. *Intersection of Paths of Symmetry-Breaking Bifurcation Points*

In a 2-parameter problem there may well be more than one path of symmetry-breaking bifurcation points and we now consider whether or not these paths can be expected to intersect. An example is given by the Bénard problem, when the bifurcating convective branch may have varying numbers of cells. The following example shows that, in general, we cannot expect intersection in paths of symmetry-breaking bifurcation points in 2-parameter problems with only $\mathbf{Z}_2$ symmetry. Consider the following problem

$$\mathbf{f}(\hat{x}, \hat{y}, \lambda, \mu) = \begin{pmatrix} \hat{x}(\hat{x}^2 - (\lambda - \mu)) \\ \hat{y}(\hat{y}^2 - (\lambda + \mu)) \end{pmatrix} = \mathbf{0}. \tag{2.11}$$

The solutions are

(1) $\hat{x} = \hat{y} = 0$ for all λ, μ,

(2) $\hat{x} = 0$, $\hat{y} = \pm\sqrt{(\lambda + \mu)}$, $\lambda + \mu > 0$,

(3) $\hat{x} = \pm\sqrt{(\lambda - \mu)}$, $\hat{y} = 0$, $\lambda - \mu > 0$,

(4) $\hat{x} = \pm\sqrt{(\lambda - \mu)}$, $\hat{y} = \pm\sqrt{(\lambda + \mu)}$, $\lambda > |\mu|$.

In solution (4) any combination of signs is possible; these branches bifurcate from the nonzero branches (2) and (3) along the line $\lambda = |\mu|$. These bifurcations are the so-called secondary bifurcations which arise near a multiple eigenvalue [8]. The $\mathbf{Z}_2$ symmetry obeyed by (2.11) is of course

$$\mathbf{f}(-\hat{x}, -\hat{y}, \lambda, \mu) = -\mathbf{f}(\hat{x}, \hat{y}, \lambda, \mu), \tag{2.12}$$

and the paths of symmetry-breaking bifurcation points are

$$\hat{x} = \hat{y} = 0, \qquad \lambda = \pm\mu. \tag{2.13}$$

We now perturb (2.11) by an arbitrary small amount, but still preserving the $\mathbf{Z}_2$ symmetry (2.12), to give the following system

$$\mathbf{f}_\varepsilon(\hat{x}, \hat{y}, \lambda, \mu) = \begin{pmatrix} \hat{x}(\hat{x}^2 - (\lambda - \mu)) + \varepsilon\hat{y} \\ \hat{y}(\hat{y}^2 - (\lambda + \mu)) + \varepsilon\hat{x} \end{pmatrix} = \mathbf{0}. \tag{2.14}$$

Equation (2.14) still has two paths of symmetry-breaking bifurcations points with $\hat{x} = \hat{y} = 0$ but they are now given by

$$\det \begin{vmatrix} -(\lambda - \mu) & \varepsilon \\ \varepsilon & -(\lambda + \mu) \end{vmatrix} = 0, \qquad \text{i.e.,} \quad \lambda^2 - \mu^2 - \varepsilon^2 = 0. \tag{2.15}$$

The solutions of (2.15) are

$$\lambda = \pm\sqrt{(\mu^2 + \varepsilon^2)}, \tag{2.16}$$

which are two curves that do not intersect, see Fig. 2.

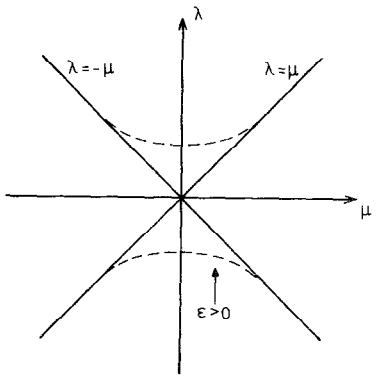

FIG. 2. The effect of a perturbation on the intersection of paths of symmetry-breaking bifurcation points, for problems with $\mathbf{Z}_2$ symmetry, where the solid line is $\varepsilon = 0$ and the dashed line is $\varepsilon > 0$.

This simple example illustrates that, in general, in a 2-parameter problem with $\mathbf{Z}_2$ symmetry a double eigenvalue corresponding to the intersection of two paths of symmetry-breaking bifurcation points is not stable when subject to small perturbations, and hence is not to be expected in a numerical calculation which always contains such perturbations. The situation is different, however, when the symmetry group is $\mathbf{Z}_2 \times \mathbf{Z}_2$. Let $\mathbf{X}_1$ and $\mathbf{X}_2$ by any distinct pair of $\mathbf{X}_{sa}$, $\mathbf{X}_{as}$, $\mathbf{X}_{aa}$ and let γ_1 and γ_2 be their corresponding symmetry operators so that $\gamma_1 \mathbf{x} = -\mathbf{x}$, $\gamma_2 \mathbf{x} = \mathbf{x}$ for $\mathbf{x} \in \mathbf{X}_1$ and $\gamma_1 \mathbf{x} = \mathbf{x}$, $\gamma_2 \mathbf{x} = -\mathbf{x}$ for $x \in \mathbf{X}_2$; we call $(\mathbf{x}_0, \lambda_0, \mu_0)$ a double symmetry-breaking bifurcation point if

$$\begin{aligned} \text{Null}(\mathbf{f}_{\mathbf{x}}^0) &= \text{Span}\{\boldsymbol{\phi}_1^0, \boldsymbol{\phi}_2^0\}, \qquad \boldsymbol{\phi}_1^0 \in \mathbf{X}_1,\ \boldsymbol{\phi}_2^0 \in \mathbf{X}_2 \\ \text{Range}(\mathbf{f}_{\mathbf{x}}^0) &= \{\mathbf{y} \in \mathbf{X} \mid \boldsymbol{\psi}_1^0 \mathbf{y} = 0 \text{ and } \boldsymbol{\psi}_2^0 \mathbf{y} = 0\}, \qquad \boldsymbol{\psi}_1^0,\ \boldsymbol{\psi}_2^0 \in \mathbf{X}' \end{aligned} \tag{2.17}$$

where

$$\boldsymbol{\psi}_1^0 \mathbf{x} = 0 \quad \text{for} \quad \mathbf{x} \in \mathbf{X}_2, \qquad \boldsymbol{\psi}_2^0 \mathbf{x} = 0 \quad \text{for} \quad \mathbf{x} \in \mathbf{X}_1$$

and

$$\boldsymbol{\psi}_1^0(\mathbf{f}_{\mathbf{x}\lambda}^0 + \mathbf{f}_{\mathbf{xx}}^0 \mathbf{v}_0)\,\boldsymbol{\phi}_1^0 \neq 0, \qquad \boldsymbol{\psi}_2^0(\mathbf{f}_{\mathbf{x}\lambda}^0 + \mathbf{f}_{\mathbf{xx}}^0 \mathbf{v}_0)\,\boldsymbol{\phi}_2^0 \neq 0$$

where

$$\mathbf{f}_{\mathbf{x}} \mathbf{v}_0 + \mathbf{f}_{\lambda} = 0, \qquad \mathbf{v}_0 \in \mathbf{X}_{ss}.$$

We now extend the notation we used for the system (2.10). Let $\mathbf{F}_{s,1}$ be $\mathbf{F}$ acting on $\mathbf{X}_{ss} \times \mathbf{X}_1 \times R$, similarly for $\mathbf{F}_{s,2}$. Let $\mathbf{F}_{s2,1}$ be $\mathbf{F}$ acting on $(\mathbf{X}_{ss} \oplus \mathbf{X}_2) \times \mathbf{X}_1 \times R$, similarly for $\mathbf{F}_{s1,2}$. Solutions to $\mathbf{F}_{s,1}$ characterize symmetry-breaking bifurcations from a completely symmetric branch (i.e., a branch lying in $\mathbf{X}_{ss}$); at such points the γ_1 symmetry is broken but the γ_2 symmetry is preserved so that the bifurcating

branch lies in $\mathbf{X}_{ss} \oplus \mathbf{X}_1$. Along a branch lying in $\mathbf{X}_{ss} \oplus \mathbf{X}_1$ the γ_2 symmetry may be broken at a symmetry-breaking bifurcation point which is the solution of $\mathbf{F}_{s1,2}$. Similar interpretations apply to the systems $\mathbf{F}_{s,2}$ and $\mathbf{F}_{s2,1}$. We note that a solution of $\mathbf{F}_{s,1}$ is always a solution of $\mathbf{F}_{s2,1}$ but that the converse is not true. The four systems $\mathbf{F}_{s,1}$, $\mathbf{F}_{s,2}$, $\mathbf{F}_{s1,2}$, and $\mathbf{F}_{s2,1}$ characterise all the possible symmetry-breaking bifurcations that can occur in this problem. We have the following theorem.

THEOREM 1. *Let* $(\mathbf{x}_0, \lambda_0, \mu_0)$ *be a double symmetry breaking bifurcation point defined by* (2.17). *Then*

(i) $\mathbf{F}_{s,1}$ and $\mathbf{F}_{s,2}$ are regular at $\mu = \mu_0$.

(ii) $\mathbf{F}_{s2,1}$ and $\mathbf{F}_{s1,2}$ have pitchfork bifurcation points at $\mu = \mu_0$ if and only if

$$\det \begin{vmatrix} \psi_1^0(\mathbf{f}_{\mathbf{x}\lambda}^0 + \mathbf{f}_{\mathbf{xx}}^0 \mathbf{v}_0)\,\phi_1^0 & \psi_1^0(\mathbf{f}_{\mathbf{x}\mu}^0 + \mathbf{f}_{\mathbf{xx}} \mathbf{w}_0)\,\phi_1^0 \\ \psi_2^0(\mathbf{f}_{\mathbf{x}\lambda}^0 + \mathbf{f}_{\mathbf{xx}}^0 \mathbf{v}_0)\,\phi_2^0 & \psi_2^0(\mathbf{f}_{\mathbf{x}\mu} + \mathbf{f}_{\mathbf{xx}} \mathbf{w}_0)\,\phi_2^0 \end{vmatrix} \neq 0 \tag{2.18}$$

where

$$\mathbf{f}_{\mathbf{x}} \mathbf{w}_0 + \mathbf{f}_\mu = 0, \qquad \mathbf{w}_0 \in \mathbf{X}_{ss}.$$

Proof. The proof of (i) is immediate. To prove (ii) one easily shows that $\mathbf{\Psi}_0 = (\psi_2, 0, 0)$ and $\mathbf{\Phi}_0 = (\phi_2, \mathbf{z}, 0)$, where $\mathbf{f}_{\mathbf{x}} \mathbf{z} + \mathbf{f}_{\mathbf{xx}} \phi_1 \phi_2 = 0$, $\mathbf{z} \in \mathbf{X}_1$, are the unique left and right eigenvectors of $\mathbf{F}_{s2,1;\mathbf{y}}^0$. The condition (2.18) can then be shown, by computation, to be equivalent to

$$\mathbf{\Psi}_0(\mathbf{F}_{s2,1;\mathbf{y}\mu}^0 + \mathbf{F}_{s2,1;\mathbf{yy}}^0 \mathbf{V}_0)\,\mathbf{\Phi}_0 \neq 0,$$

where

$$\mathbf{F}_{s2,1;\mathbf{y}}^0 \mathbf{V}_0 + \mathbf{F}_{s2,1;\mu} = 0.$$

It is easy to check that

$$\mathbf{\Psi}_0 \mathbf{F}_{s2,1;\mathbf{yy}} \mathbf{\Phi}_0 \mathbf{\Phi}_0 = 0$$

and

$$\mathbf{\Psi}_0 \mathbf{F}_{s2,1;\mu} = 0.$$

Similarly for $\mathbf{F}_{s1,2}$. ∎

Using the implicit function theorem and part (i) of the above theorem shows that two paths of symmetry-breaking bifurcation points intersect at a double symmetry-breaking bifurcation point and one can easily check that the angle between these paths is nonzero if and only if condition (2.18) is satisfied. Near a double singular point a variety of behaviour is possible depending on the direction (sub- or super-critical) of the various bifurcations. All of it will of course be consistent with

Theorem 1. In Figs. 3a and 3b we give an illustration of the theorem. In this example all the symmetry-breaking bifurcations of the basic equations are supercritical. Figure 3a shows the projection on the $(\lambda - \mu)$ plane of the various bifurcations. The two paths on which $\mathbf{F}_{s2,1}$ and $\mathbf{F}_{s1,2} = 0$ are paths of secondary bifurcations which necessarily arise at bifurcation at a multiple eigenvalue [8]. These paths are the bifurcating solution branches of the systems $\mathbf{F}_{s2,1}$ and $\mathbf{F}_{s1,2}$ which arise from the pitchfork bifurcation point in these systems (Theorem 1(ii)) at $(\lambda_0 \mu_0)$. Figure 3b shows a state diagram for $\mu > \mu_0$. The two functionals l_1 and l_2 are such that $l_1(\mathbf{x}) = 0$ for $\mathbf{x} \in \mathbf{X}_2$ and $l_2(\mathbf{x}) = 0$ for $\mathbf{x} \in \mathbf{X}_1$, so that they measure the component of the solution in the spaces $\mathbf{X}_1$ and $\mathbf{X}_2$, respectively.

Finally we introduce the following extended system which could be used to compute, numerically, double symmetry-breaking bifurcation points (cf. Werner [7, Eq. (4.9)]

$$\mathbf{H}(\mathbf{s}) = \begin{pmatrix} \mathbf{f}_{\mathbf{x}}(\mathbf{x}, \lambda, \mu) \\ \mathbf{f}_{\mathbf{x}}(\mathbf{x}, \lambda, \mu)\, \boldsymbol{\phi}_1 \\ \mathbf{f}_{\mathbf{x}}(\mathbf{x}, \lambda, \mu)\, \boldsymbol{\phi}_2 \\ l_1 \boldsymbol{\phi}_1 - 1 \\ l_2 \boldsymbol{\phi}_2 - 1 \end{pmatrix} = \mathbf{0}, \qquad \begin{aligned} &\mathbf{s} = (\mathbf{x}, \boldsymbol{\phi}_1, \boldsymbol{\phi}_2, \lambda, \mu) \in \mathbf{Z} \\ &\mathbf{Z} = \mathbf{X}_{ss} \times \mathbf{X}_1 \times \mathbf{X}_2 \times R \times R \\ &\mathbf{H}: \mathbf{Z} \to \mathbf{Z}. \end{aligned} \tag{2.20}$$

Using the methods of Werner and Spence [6] and Werner [7] one can prove the following theorem.

THEOREM 2. *Let* $(\mathbf{x}_0, \lambda_0, \mu_0)$ *be a double symmetry-breaking bifurcation point of* $\mathbf{f}$. *Then* (2.20) *has an isolated solution if and only if* (2.18) *is satisfied.*

The main consequence of this theorem here is that double symmetry-breaking points are stable to perturbations which preserve the $\mathbf{Z}_2 \times \mathbf{Z}_2$ symmetry.

To summarize then, we have shown in this section that two paths of symmetry-breaking bifurcation points which break a different symmetry in each case may cross in a stable way in a 2-parameter problem. If however the same symmetry is broken on each path then we would not expect them to cross.

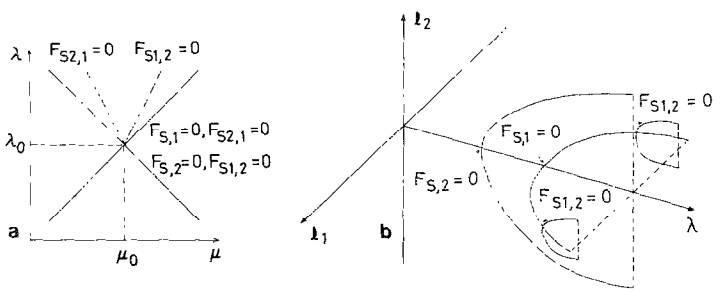

FIG. 3. (a) Two paths of symmetry-breaking bifurcation points, for problems with $\mathbf{Z}_2 \times \mathbf{Z}_2$ symmetry, and the two paths of secondary bifurcations which arise at their intersection. (b) The state diagram corresponding to Fig. 3a for a fixed value of $\mu > \mu_0$.

3. Equations and Finite-Element Method

We are considering 2-dimensional convection in a box of height H and width L. We use cartesian coordinates x^* and y^* and denote the velocity by $\mathbf{u}^* \equiv (u_1^*, u_2^*)$, and the temperature and pressure by T^* and p^*. The natural convection is described by the steady Navier–Stokes and energy equations which we solve in the Boussinesq approximation. This approximation neglects all variation of fluid properties, except for the change in density which gives rise to the buoyancy force for which a linear dependence of density on temperature is assumed. The equations become

$$\beta u_1 \frac{\partial u_1}{\partial x} - u_2 \frac{\partial u_1}{\partial y} + \beta \frac{\partial p}{\partial x} - \mathrm{Pr}\left\{\beta^2 \frac{\partial^2 u_1}{\partial x^2} + \frac{\partial^2 u_1}{\partial y^2}\right\} = 0, \tag{3.1}$$

$$\beta u_1 \frac{\partial u_2}{\partial x} + u_2 \frac{\partial u_2}{\partial y} + \frac{\partial p}{\partial y} - \mathrm{Pr}\left\{\beta^2 \frac{\partial^2 u_2}{\partial x^2} + \frac{\partial^2 u_2}{\partial y^2}\right\} = \mathrm{RaPr}\, T, \tag{3.2}$$

$$\beta \frac{\partial u_1}{\partial x} + \frac{\partial u_2}{\partial y} = 0, \tag{3.3}$$

$$\beta u_1 \frac{\partial T}{\partial x} + u_2 \frac{\partial T}{\partial y} - u_2 - \left\{\beta^2 \frac{\partial^2 T}{\partial x^2} + \frac{\partial^2 T}{\partial y^2}\right\} = 0. \tag{3.4}$$

In the above equations x, y, $\mathbf{u}$, p, and T are given by

$$x = \frac{x^*}{L}, \qquad y = \frac{y^*}{H}, \qquad \mathbf{u} = \frac{\mathbf{u}^*}{K/H}, \qquad p = \frac{p^*}{\rho_0 K^2/H^2} - \mathrm{RaPr}\left(y - \frac{y^2}{2}\right)$$

$$T = \frac{T^* - T_c^*}{T_h^* - T_c^*} - \left(\frac{1}{2} - y\right),$$

where $\beta = L/H$, $\mathrm{Ra} = g\alpha(T_h^* - T_c^*)\, L^3/Kv$, $\mathrm{Pr} = v/K$. T_c^* and T_h^* are the temperatures of the top and bottom of the box, α is the coefficient of volumetric expansion of the fluid, K is its thermal diffusivity and v its kinematic viscosity. The density at some reference temperature, T_c^* say, is denoted by ρ_0 and g is the gravitational acceleration. The term RaPr T on the right-hand side of Eq. (3.2) is the buoyancy force which arises from the linearised density variation assumed in the Boussinesq approximation.

Equations (3.1)–(3.4) hold in the region

$$D = \{(x, y) \mid -\tfrac{1}{2} \leqslant x \leqslant \tfrac{1}{2},\ -\tfrac{1}{2} \leqslant y \leqslant \tfrac{1}{2}\}.$$

The boundary conditions are that u_1 and u_2 are zero on the whole boundary of D and T is zero on $y = \pm\frac{1}{2}$ with $\partial T/\partial x = 0$ on $x = \pm\frac{1}{2}$. These equations admit the trivial conducting solution $u_1 = u_2 = p = T = 0$. (Note that T is the non-dimensional temperature perturbation.)

It is convenient to convert Eqs. (3.1)–(3.4) and the boundary conditions into an operator equation in an appropriate Hilbert space. We introduce the following notation: let $L^2(D)$ be the space of functions which are square integrable over D; let $W^{1,2}(D)$ be the space of functions whose generalized first derivatives lie in $L^2(D)$. Let $W_0^{1,2}(D)$ be that subspace of $W^{1,2}(D)$ whose elements vanish (weakly) on the boundary of D and let $W_T^{1,2}(D)$ be the subspace whose elements vanish weakly on $y = \pm\frac{1}{2}$. $W^{1,2}(D)^2$ is the space of vector-valued functions each component of which is in $W^{1,2}(D)$. Finally let $\mathbf{H} = W_0^{1,2}(D)^2 \times L^2(D) \times W_T^{1,2}(D)$. We introduce the following functionals

$$a(\mathbf{U}; \mathbf{V}, \mathbf{W}) = \int_D \left[\left(\beta u_1 \frac{\partial v_1}{\partial x} + u_2 \frac{\partial v_1}{\partial y} \right) w_1 + \left(\beta u_1 \frac{\partial v_2}{\partial x} + u_2 \frac{\partial v_2}{\partial y} \right) w_2 + \left(\beta u_1 \frac{\partial R}{\partial x} + u_2 \frac{\partial R}{\partial y} \right) S \right] \tag{3.5a}$$

$$b(\mathbf{U}, \mathbf{W}) = \int_D \left[\mathrm{Pr} \left(\beta^2 \frac{\partial u_1}{\partial x} \frac{\partial w_1}{\partial x} + \frac{\partial u_1}{\partial y} \frac{\partial w_1}{\partial y} + \beta^2 \frac{\partial u_2}{dx} \frac{\partial w_2}{\partial x} + \frac{\partial u_2}{\partial y} \frac{\partial v_2}{\partial y} \right] + \beta^2 \frac{\partial T}{\partial x} \frac{\partial S}{\partial x} + \frac{\partial T}{\partial y} \frac{\partial S}{\partial y} - \mathrm{Ra}\ \mathrm{Pr}\ T w_2 - u_2 S \right]$$

$$- \int_D \left[p \left(\beta \frac{\partial w_1}{\partial x} + \frac{\partial w_2}{\partial y} \right) + r \left(\beta \frac{\partial u_1}{\partial x} + \frac{\partial u_2}{\partial y} \right) \right] \tag{3.5b}$$

where $\mathbf{U} = (u_1, u_2, p, T)$, $\mathbf{V} = (v_1, v_2, q, R)$, and $\mathbf{W} = (w_1, w_2, r, S)$ with $\mathbf{U}, \mathbf{V}, \mathbf{W} \in \mathbf{H}$.

We now define the operator

$$\mathbf{A}: \mathbf{H} \times R \times R \to \mathbf{H},$$

by

$$\mathbf{A}(\mathbf{U}, \mathrm{Ra}, \beta) = \mathbf{W},$$

where

$$a(\mathbf{U}; \mathbf{U}, \mathbf{V}) + b(\mathbf{U}, \mathbf{V}) = \langle \mathbf{W}, \mathbf{V} \rangle \qquad \text{for all} \quad \mathbf{V} \in \mathbf{H}. \tag{3.6}$$

and $\langle \cdot, \cdot \rangle$ denotes the inner product in the Hilbert space $\mathbf{H}$. For fixed $\mathbf{U}$ the right-hand side of (3.6) defines a bounded linear functional on $\mathbf{H}$, which by the Reisz representation theorem means $\mathbf{W}$ exists, and thus $\mathbf{A}$ is well defined. A classical solution of (3.1)–(3.4) satisfies

$$\mathbf{A}(\mathbf{U}, \mathrm{Ra}, \beta) = 0. \tag{3.7}$$

Solutions of (3.7) are called weak or generalized solutions and may, under certain smoothness conditions, be shown to be classical solutions of (3.1)–(3.4). The weak

form of Eqs. (3.1)–(3.4) given by (3.7) is convenient for studying the effects of the symmetry on both the continuous and discrete (finite-element) versions of the problem.

We now consider the symmetry properties of **A**. Define S_x, $S_y \in \mathscr{L}(\mathbf{H})$ by

$$\begin{aligned} S_x\mathbf{U} &\equiv S_x(u_1(x, y), u_2(x, y), p(x, y), T(x, y)) \\ &= (u_1(x, -y), -u_2(x, -y), p(x, -y), -T(x, -y)) \end{aligned} \tag{3.8}$$

$$\begin{aligned} S_y\mathbf{U} &\equiv S_y(u_1(x, y), u_2(x, y), p(x, y), T(x, y)) \\ &= (-u_1(-x, y), u_2(-x, y), p(-x, y), T(-x, y)), \end{aligned} \tag{3.9}$$

for smooth functions, and use continuity to extend the definition to the whole space. Clearly S_x represents reflection about the x-axis and S_y represents reflection about the y axis. We also note that

$$S_xS_y\mathbf{U} = S_yS_x\mathbf{U} \qquad \text{for all} \quad \mathbf{U} \in \mathbf{H}. \tag{3.10}$$

A simple change of variable in the integrals in (3.5) gives the following

$$\begin{aligned} a(S_x\mathbf{U}; S_x\mathbf{V}, \mathbf{W}) &= a(\mathbf{U}: \mathbf{V}, S_x\mathbf{W}) \\ b(S_x\mathbf{U}, \mathbf{W}) &= b(\mathbf{U}, S_x\mathbf{W}) \end{aligned} \tag{3.11}$$

$$\begin{aligned} a(S_y\mathbf{U}; S_y\mathbf{V}, \mathbf{W}) &= a(\mathbf{U}; \mathbf{V}, S_y\mathbf{W}) \\ b(S_y\mathbf{U}, \mathbf{W}) &= b(\mathbf{U}, S_y\mathbf{W}). \end{aligned} \tag{3.12}$$

Similarly we have

$$\langle S_x\mathbf{U}, \mathbf{V}\rangle = \langle \mathbf{U}, S_x\mathbf{V}\rangle, \tag{3.13}$$

$$\langle S_y\mathbf{U}, \mathbf{V}\rangle = \langle \mathbf{U}, S_y\mathbf{V}\rangle. \tag{3.14}$$

Let $\Gamma = \{I, S_x, S_y, S_xS_y\}$ which is a representation of $\mathbf{Z}_2 \times \mathbf{Z}_2$ over **H**. Using (3.6) and (3.8)–(3.14) we can show that (cf. (2.2) in Sect. 2):

PROPOSITION 1. *For* **A** *defined by* (3.6),

$$\mathbf{A}(\gamma\mathbf{U}, \mathrm{Ra}, \beta) = \gamma\mathbf{A}(\mathbf{U}, \mathrm{Ra}, \beta) \qquad \text{for all } \gamma \in \Gamma, \mathbf{U} \in \mathbf{H}, \mathrm{Ra}, \beta \in R. \tag{3.15}$$

Thus the theory described in the previous section applies to the convection problem we are considering here. We define the region D^+ by

$$D^+ = \{(x, y) \mid 0 \leqslant x \leqslant \tfrac{1}{2}, 0 \leqslant y \leqslant \tfrac{1}{2}\}.$$

It is easy to show, using change of variables in the integrals in (3.5), that the following holds

$$a(\mathbf{U};\mathbf{V},\mathbf{W}) = a^+(\mathbf{U};\mathbf{V},\mathbf{W}) + a^+(S_x\mathbf{U};S_x\mathbf{V},S_x\mathbf{W}) + a^+(S_y\mathbf{U};S_y\mathbf{V},S_y\mathbf{W}) + a^+(S_xS_y\mathbf{U};S_xS_y\mathbf{V},S_xS_y\mathbf{W}) \tag{3.16}$$

where a^+ is defined as in (3.5) but with the region of integration D replaced by D^+.

Using the results of the last section a symmetry-breaking bifurcation point of (3.7) corresponds to an isolated solution of

$$\begin{pmatrix} \mathbf{A}(\mathbf{U},\mathrm{Ra},\beta) \\ D\mathbf{A}(\mathbf{U},\mathrm{Ra},\beta)\,\boldsymbol{\Phi} \\ l\boldsymbol{\Phi}-1 \end{pmatrix} = 0 \tag{3.17}$$

where

$$\mathbf{U}\in\{\mathbf{U}\in\mathbf{H}\mid S_x\mathbf{U}=\mathbf{U},\ S_y\mathbf{U}=\mathbf{U}\},$$

$$\boldsymbol{\Phi}\in\{\boldsymbol{\Phi}\in\mathbf{H}\mid \gamma_1\boldsymbol{\Phi}=-\boldsymbol{\Phi},\ \gamma_2\boldsymbol{\Phi}=-\boldsymbol{\Phi},\ \gamma_3\boldsymbol{\Phi}=\boldsymbol{\Phi}\},$$

with $\{\gamma_1,\gamma_2,\gamma_3\}=\{S_x,S_y,S_{xy}\}$ and l is a normalization of $\boldsymbol{\Phi}$. The Fréchet derivative of $\mathbf{A}$, $D\mathbf{A}$, is defined by

$$D\mathbf{A}(\mathbf{U},Ra,\beta)\,\boldsymbol{\Phi}=\mathbf{W}$$

where

$$a(\mathbf{U};\boldsymbol{\Phi},\mathbf{V})+a(\boldsymbol{\Phi};\mathbf{U},\mathbf{V})+b(\boldsymbol{\Phi},\mathbf{V})=\langle\mathbf{W},\mathbf{V}\rangle \qquad \text{for all}\quad \mathbf{V}\in\mathbf{H}. \tag{3.18}$$

The crucial point is that since $\mathbf{U}$ and $\boldsymbol{\Phi}$ are eigenvectors of all the symmetry operators in Γ, Eq. (3.16) may be used to express all the integrals in (3.17) as integrals over D^+. Thus we need only discretize the region D^+ and this reduces the number of freedoms in the problem by a factor of approximately 4 in two dimensions.

We used a Galerkin finite-element method to discretize the equations. This is done by replacing the space $\mathbf{H}$ by a finite-dimensional subspace $\mathbf{H}_h$. We used 9-noded quadrilateral elements with biquadratic interpolation for the velocities and temperature and piecewise linear, discontinuous, interpolation for the pressure. Provided the finite-element mesh is symmetric with respect to reflection about the x and y axes all the theory given in this section applies equally to the discretization, essentially because $\mathbf{H}_h\subset\mathbf{H}$. (For further details see the paper by Cliffe and Spence [16]). The Newton method of solution of the discrete version of (3.17) is described in detail by Werner and Spence [6]. We mention that this involves two LU factorizations (essentially of the symmetric and antisymmetric Jacobian

matrices) and the solution of three linear systems of equations. The LU factorizations and subsequent solutions were carried out using the frontal method [9]. The matrices have a banded structure with one of them having, in addition, a full column. This is handled automatically by the frontal procedure by keeping the variable corresponding to the full column in core throughout the factorization procedure. The penalty for this is minimal. The frontal method we used employs partial pivoting [9] and we encountered no problems with singularities or ill-conditioning.

4. Results

The algorithms developed in the previous section will now be applied to Bénard convection in a 2-dimensional cavity. The geometry is shown is Fig. 4; a fluid is confined between rigid horizontal surfaces and rigid sidewalls. It is heated by maintaining its lower surface at a constant, higher temperature than the upper one. Heat is transferred by conduction for Rayleigh numbers below a critical value Ra_1, and there is no-flow equilibrium state which is stable; any perturbations are suppressed by the action of thermal conductivity and viscosity which restores the equilibrium. However, for Rayleigh numbers greater than Ra_1, the restoring forces are insufficient to overcome the buoyancy generated by perturbations and the equilibrium is unstable; the perturbations grow and steady convection results. For a cavity of aspect ratio one, this flow consists of a single cell and because of the vertical symmetry of the problem there are two possible senses of rotation for this cell.

The trivial, no-flow state is in fact a solution of the steady state equation for all values of Ra (although it is unstable above Ra_1), and there are successive bifurcations from the trivial branch. For example, the second bifurcation at Ra_2 corresponds to a 2-cell solution for an aspect ratio of one. These bifurcation points move as the aspect ratio varies, and trace paths in the 2-parameter space formed by the Rayleigh number and aspect ratio. The considerations of the previous section allow us to predict that only paths of bifurcation points which break different sym-

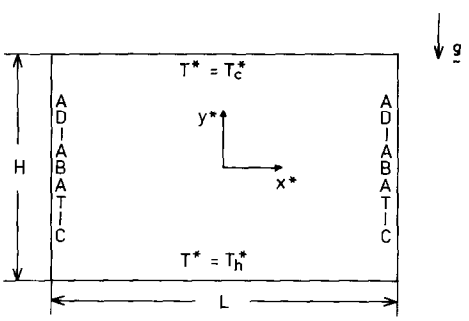

FIG. 4. The geometry for confined Bénard convection. All surfaces are rigid.

metries will cross. Thus, as the aspect ratio increases from one, the path of points representing bifurcation to a 1-cell solution will intersect that corresponding to bifurcation to a 2-cell solution, since the 1-cell solution breaks both horizontal and vertical symmetries while the 2-cell solution breaks only the horizontal symmetry. On the other hand, the path of 1-cell bifurcation points will not intersect that corresponding to bifurcation to three cells, since they both break the same horizontal and vertical symmetries. Instead the paths are expected to approach and recede, gradually exchanging identities so that the 1-cell bifurcation point develops smoothly into a 3-cell point. This phenomenon was observed, but not explained correctly, by Jackson and Winters [10] in a finite-element study of the Bénard problem. Their results are shown in Fig. 5, where the numbers show the number of cells which develop from the bifurcation point. It is worth noting that in the related problem of Bénard convection in a cylinder, the same symmetry is always broken by each bifurcation point, and no paths are expected to cross as observed by Brown, Yamaguchi, and Chang [11].

4.1. *Extended Systems*

The Werner–Spence algorithm and that for bifurcation from the trivial solution were applied to the Bénard problem. The calculations were carried out over a quarter of the domain for bifurcation both to an odd and an even number of cells. In

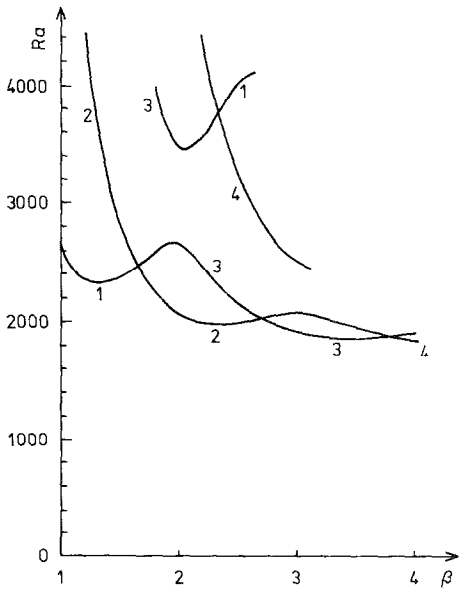

FIG. 5. The paths of symmetry-breaking bifurcation points for the confined Bénard problem, as the aspect ratio β varies [10]. The curves are labelled by the number of cells which develop from the bifurcation point.

each case, the same boundary conditions were applied to the solution $\mathbf{U}$ on the inner boundaries, namely

(i) horizontal axis ($y=0$): $\partial u_1/\partial y = \partial p/\partial y = 0$, $u_2 = T = 0$.
(ii) vertical axis ($x=0$): $u_1 = 0$, $\partial u_2/\partial x = \partial p/\partial x = \partial T/\partial x = 0$.

In the case of an odd number of cells, both horizontal and vertical symmetries are broken, that is the eigenvector $\mathbf{\Phi}$ satisfies

$$S_x\mathbf{\Phi} = -\mathbf{\Phi}, \qquad S_y\mathbf{\Phi} = -\mathbf{\Phi}, \qquad \text{and} \qquad S_{xy}\mathbf{\Phi} = \mathbf{\Phi}.$$

The boundary conditions for $\mathbf{\Phi} = (\phi_1, \phi_2, \pi, \theta)$ are then

(i) horizontal axis ($y=0$): $\phi_1 = \pi = 0$, $\partial\phi_2/\partial y = \partial\theta/\partial y = 0$.
(ii) vertical axis ($x=0$): $\partial\phi_1/\partial x = 0$, $\phi_2 = \pi = \theta = 0$.

For bifurcation to an even number of cells, only the horizontal symmetry is broken, that is,

$$S_x\mathbf{\Phi} = -\mathbf{\Phi}, \qquad S_y\mathbf{\Phi} = \mathbf{\Phi}, \qquad \text{and} \qquad S_{xy}\mathbf{\Phi} = -\mathbf{\Phi}.$$

The boundary conditions for $\mathbf{\Phi}$ become

(i) horizontal axis ($y=0$): $\phi_1 = \pi = 0$, $\partial\phi_2/\partial y = \partial\theta/\partial y = 0$.
(ii) vertical axis ($x=0$): $\phi_1 = 0$, $\partial\phi_2/\partial x = \partial\pi/\partial x = \partial\theta/\partial x = 0$.

It is important to note that we are effectively solving the problem on a quarter of the domain with the symmetry conditions being handled by appropriate boundary conditions on the symmetry axes. In particular, no special elements are required and no symmetry need be imposed on the elements (it is implicit that the discretization of the full domain is generated by reflecting first about the x axis and then about the y axis or equivalently the reflections may be carried out in reverse order).

The Navier–Stokes equations were solved for values of the width-to-height ratio from 1.0 to 3.0 in steps of 0.2 using a grid of 2×2 elements. The computational time for these 11 solutions was found to be 6.6 s using the Werner–Spence algorithm. The same calculation was found to take 66.2 s with the Moore algorithm over the full domain on a grid of 4×4 elements (Cliffe and Winters [2]). Although the Werner–Spence algorithm has a factor of four fewer degrees of freedom than the Moore system, a much greater reduction in cost arises here due to the use of the frontal method for solving the matrix equations.

The system for predicting bifurcation from the trivial solution was found to give a further reduction in cost of one half, the 11 bifurcation points being computed in 3.2 s, a factor of over 20 faster than obtained with the Moore algorithm.

4.2. *Choice of Finite Element*

The trivial, no-flow solution of the Boussinesq equations corresponds to a simple balance between buoyancy term and pressure gradient. The requirement of mixed interpolation forces us to use a lower order of interpolation for the pressure than for the temperature and velocity. The result is that it may not be possible to satisfy exactly the balance between pressure gradient and buoyancy. Gresho et al. [13] demonstrated, for example, that the 9-node element with bilinear pressure approximation gives rise to a spurious momentum source, and suggested the use of an element with discontinuous pressure approximation. Cliffe, Jackson, and Winters [14] proposed an alternative element with discontinuous pressure approximation and showed that it was able to satisfy exactly the pressure gradient–buoyancy balance. In the context of their work, this allowed natural convection at very high Rayleigh numbers to be computed.

All the present calculations were carried out with the discontinuous pressure element of Cliffe, Jackson, and Winters [14] and Table I shows that this gives excellent agreement with an independent calculation, using a different method, by Luijkx and Platten [15]. The table also gives the finite-element predictions of Cliffe and Winters [2] using a grid of 4×4 elements with continuous, linear pressure approximation over the full domain. The spurious momentum source produced by this element gives rise to an error of up to 2%. A similar error is present in the work of Jackson and Winters [10] and explains the discrepancy between their results and Luijkx and Platten [15]. It should to be noted that the present grid of 2×2 elements over the quarter-domain is clearly inadequate when predicting accurately the bifurcation to 3 cell flow at the largest aspect ratios of 2.8 and 3.0.

TABLE I

Lowest Critical Rayleigh Number for Bifurcation to an Odd-Cell Flow for Different Aspect Ratios

Aspect ratio β	Present results	Luijkx and Platten [15]	Cliffe and Winters [2]
1.0	2594	2585	2651
1.2	2296	2291	2345
1.4	2277	2275	2322
1.6	2392	2393	2435
1.8	2550	—	2589
2.0	2546	—	2563
2.2	2278	—	2250
2.4	2031	—	1959
2.6	1856	—	1740
2.8	1736	1928	1576
3.0	1657	1871	1450

5. Conclusions

A recently proposed method for finding symmetry-breaking points has been implemented in a finite-element formulation and applied to 2-dimensional Bénard convection in a finite cavity. It was found to reduce the computational cost by a factor of ten when compared with an earlier method which does not exploit the symmetry of the problem. It was shown that a further factor of two may be obtained for those cases where bifurcation is from the trivial solution, as in Bénard convection.

When a second parameter is varied, bifurcation points trace out paths in a 2-parameter space which may or may not intersect with one another. A criterion has been established for deciding whether or not paths of symmetry-breaking bifurcation points are able to cross in a stable way.

Finally, it was shown that in the finite-element method, most commonly used elements give rise to a spurious momentum source that leads to systematic error in predictions of the critical Rayleigh number. A method for overcoming this was demonstrated.

References

1. K. A. Cliffe and K. H. Winters, *J. Comput. Phys.* **54**, 531 (1984).
2. K. A. Cliffe, and K. H. Winters, Harwell Report AERE-M. 3352, 1983 (Unpublished).
3. K. A. Cliffe, *J. Fluid Mech.* **135**, 219 (1983).
4. K. H. Winters and R. C. G. Brindley, Harwell Report AERE-R. 11373, 1984, (Unpublished).
5. G. Moore, *Numer. Funct. Anal. Optim.* **2**, 441 (1980).
6. B. Werner and A. Spence, *SIAM J. Numer. Anal.* **21**, (1984).
7. B. Werner, in *Numerical Methods for Bifurcation Problems*, (T. Küpper, H. D. Mittleman, and H. Weber, Eds.), Internat. Ser. Numer. Math. (Birkhäuser, Basel, 1984).
8. L. Bauer, H. B. Keller, and E. L. Reiss, *SIAM Rev.* **17**, 101 (1975).
9. I. S. Duff, Harwell Report AERE-R. 10079, 1981 (Unpublished).
10. C. P. Jackson and K. H. Winters, *Int. J. Numer. Methods Fluids* **4**, 127 (1984).
11. R. A. Brown, Y. Yamaguchi, and C. J. Chang, in *Proceedings, 9th National Congress of Theoretical and Applied Mechanics, 1983.*
12. K. A. Cliffe and A. Spence, *Methods for Bifurcation Problems*, (T. Küpper, H. D. Mittleman and H. Weber, Eds.), Internat. Ser. Numer. Math. (Birkhäuser, Basel, 1984).
13. P. M. Gresho, R. L. Lee. S. T. Chan, and J. M. Leone, in *Proceedings, Third Int. Conf. on Finite Elements in Flow Problems, Banff, Canada, 1980.*
14. K. A. Cliffe, C. P. Jackson and K. H. Winters, Harwell Report AERE TP. 1037, 1984 (Unpublished); *J. Comput. Phys.* **60**. 155 (1985).
15. J. Luijkx and J. K. Platten, J. Non-Equilib. Thermodyn. **6**, 141 (1981).
16. K. A. Cliffe, and A. Spence, *Proceedings, ICFD Conference on Numerical Methods for Fluid Dynamics, April 1985, Reading.*